Reconfigurable Optical Interconnection System based on the Optical Superprism Effect in Photonic Crystals

W. Pijitrojana
Department of Electrical Engineering, Faculty of Engineering,
Thammasat University, Klong Luang, Pathum Thani 12121, Thailand
Phone 0-2564-3001-9 Ext. 3045, Fax 0-2564-3010,
E-mail: pwanchai@engr.tu.ac.th

Abstract

A conceptual design of the reconfigurable optical interconnection system constructed using photonic crystals with superprism effect is proposed in this paper. Its innovative optical configuration resulted in superior optical performance. This paper describes a 16×16 reconfigurable optical transpose interconnection system architecture based on the optical superprism effect in photonic crystals. The system also follows the scaling laws of the optical system.

Keywords: Superprism effect, Planar photonic crystals, optical interconnection

1. Introduction

Chip-to-chip wiring by means of optical interconnection has focused on free space interconnection by using holograms. Lenses and interconnection by means of optical waveguide and optical fiber, have also been examined. It has been possible to parallel switch over wiring using a spatial light modulator and optical switching array as key devices in optical interconnection, and as a result, a high-density and large bandwidth optical signal processing system, which is beyond conventional wiring technology, can be achieved [1,2]. This research offers a new proposal with regard to methods that can control connecting patterns of optical interconnection by means of using photonic crystals with superprism effect. Photonic Crystals (PC's) are artificial structures, which have a periodic dielectric structure with high index contrast, designed to control photons in the same way that conventional crystals in solids control electrons. They also exhibit a complete photonic band gap (PBG)-the inhibition of spontaneous emission of light from atoms and molecules [3]. One attractive application of photonic crystals is based on using a wide deflection of a ight beam inside of the PCs by means of a slight change of the wavelength or the angle of incidence. This phenomenon was studied experimentally in [4] and investigated numerically by the finite difference time domain (FDTD) [7].

In section 2, the concepts of the superprism and the dispersion surface are reviewed. Also in section 2, the PC model with superprism effect and calculation methods are explained and used to provide a conceptual design of devices for a new reconfigurable optical interconnection system. The new conceptual design of reconfigurable optical transpose interconnection system architecture, which is based on the static optical transpose interconnection system architecture [8], is described in section 3 as well as a new conceptual architecture of the system. Finally, the comparison to the conventional system is discussed in section 4.

2. Superprism Effect and Device Design

Recently, Kosaka *et al.* demonstrated a highly dispersive photonic microstructure in a 3-D ("autocloned") PC, which was termed optical "superprism" [4,9-10]. The "autocloned" structure has very favorable properties, but requires specialized nonstandard fabrication techniques. Furthermore, the nature of the superprism effect does not require 3-D periodicity, and similar effects can be observed in 1-D and 2-D systems [11]. Moreover, the

autocloned approach does not describe guided waves but rather beam propagation in a bulk-inhomogeneous-material. This will limit the usefulness of their structure for fabricating compact systems [12].

The basis for the superprism phenomena is anisotropy in the photonic band structure, a feature which is strongly present at frequencies near the photonic band gap. The effect is very sensitive to the particular choice of incident angle relative to the orientation of the photonic crystal, as well as the incident wavelength. The anisotropy can be seen more clearly in the dispersion surfaces [10]. The surfaces correspond to index ellipsoids in conventional crystalline optics, where the length from the surface to the Γ point corresponds to the refractive index. The dispersion surfaces in PCs show a variety of shapes in contrast to the circular or ellipsoidal shapes in conventional crystals. As an example, dispersion surfaces at the frequency cut of $\Omega = 0.42$ (the frequency ω was normalized by the lateral lattice constant a as $\Omega = \omega a/2\pi c$) for TE modes are shown in Fig. 2. The surface marked A (corresponding to the band marked A in Fig. 1) showed an almost circular shape, that marked B (corresponding to the band marked B in Fig. 1) showed a strong star-shaped anisotropy. The apparent distortion from the circular shape and the multiplicity of the dispersion surface are the origins of the anisotropy phenomena.

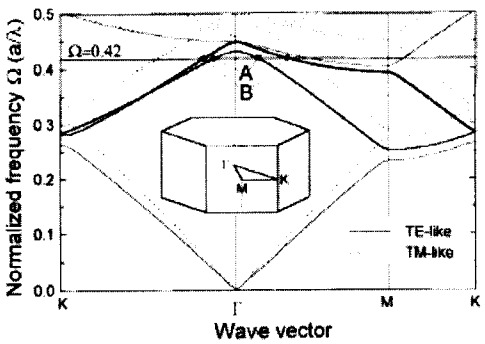

Fig. 1. Photonic in-plane band structure for the PC's used in this demonstration. A plane-wave expansion method was used. The shape of the photonic atoms was approximated as a hexagonal disk with a diameter of $0.4a$, and the refractive indexes for Si and SiO_2 were set to the measured values 3.24 and 1.46, respectively. The solid and dashed curves denote the TE-like and TM-like modes, respectively [4].

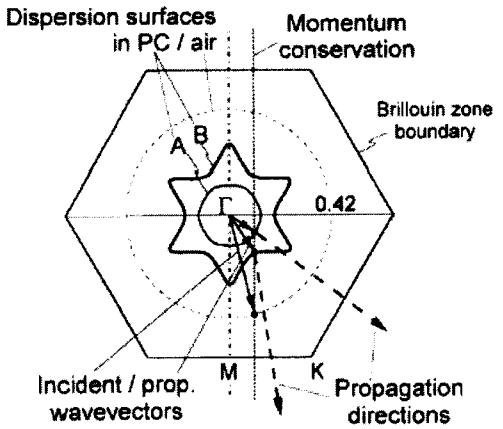

Fig. 2. Equi-frequency contours called dispersion surfaces at the frequency cut of $\Omega = 0.42$ for TE modes. The process used to derive the propagation direction is shown: the normal vector at the intersection of the dispersion surface and the construction line (through the end of the incident wavevector and normal to the crystal edge) give the propagation direction.

The process for obtaining the propagation direction from these dispersion surfaces is graphically illustrated in Fig. 2 [4]. The propagation direction is determined by the energy velocity, which is exactly the same as the group velocity v_g in a periodically distributed material without losses. The following well-known relation:

$$v_g = \nabla_\kappa \omega(\kappa) \tag{1}$$

means the group velocity points to the gradient direction of dispersion surfaces at a wavevector k. When a Gaussian beam incidents to a PC, the light propagating in the PCs is no longer a Gaussian beam. Since each plane-wave component is expanded into Bloch waves at the input end of the PC and affected by the complex dispersion characteristic. The beam width $2w$ in the PC far from the input end is expressed as:

$$2w \cong 2\frac{\lambda L}{\pi w_0} p \tag{2}$$

where p is defined as $p \equiv (\partial\theta_c/\partial\theta_i)$ for the incident beam angle θ_i and the propagating beam angle in the PC θ_c. This parameter represents the beam collimating ability in the PC. From eq. (2), L is the distance from the input end, which satisfies:

$$L > \frac{\pi w_0^2}{\lambda} p^{-1} \tag{3}$$

Since the beam width in eq. (2) occupies the far-field angle $2w/L$, the wavelength resolution is given by:

$$\frac{\Delta\lambda}{\lambda} = \frac{\left(\frac{2w}{L}\right)}{\left(\frac{a}{\lambda}\right)} \frac{\partial\left(\frac{a}{\lambda}\right)}{\partial\theta_c} \cong \frac{2\lambda^2}{\pi m w_0 a}\left(\frac{q}{p}\right)^{-1} \qquad (4)$$

where a is the lattice constant of the PC, and q is defined as $q \equiv \partial\theta_c/\partial(a/\lambda)$. This parameter represents the angle dispersion (wavelength sensitivity) of the PC. The q/p is the resolution parameter.

Fig. 3 shows two different types of superprisms in real space and $\boldsymbol{k}$ space. They use 2-D PC to confine and manipulate the light in-plane and total internal reflection to confine light vertically [5]. The result from [6] showed that a superprism could realize a sufficiently high resolution usable for the dense WDM, but that the PC cannot still be miniaturized to less than 1 cm^2.

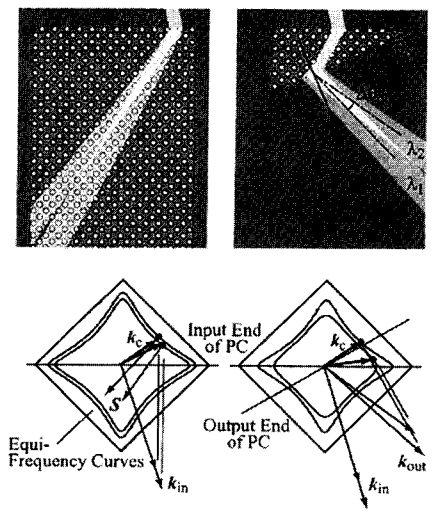

Fig. 3. Two different types of superprisms in real space and $\boldsymbol{k}$ space. 2-D PC is composed of airholes with square lattice rotated by 45°.

3. A new conceptual architecture of the system

A new conceptual architecture of the reconfigurable optical interconnection system is based on the static optical transpose interconnection system architecture [8]. The static OTIS is a one-to-one mapping between $N \times M$ input to $N \times M$ output beamlets. The input and output beamlets are arranged as an $\sqrt{N} \times \sqrt{M}$ array of $\sqrt{N} \times \sqrt{M}$ sub-arrays. Each $\sqrt{N} \times \sqrt{M}$ sub-array of input and output beamlets are at the front and back focal planes of each of the lenses of stage I and III which are arranged as an $\sqrt{N} \times \sqrt{M}$ array, respectively. Each input and output beamlets has a coordinate (n,m) where $n,m = 1,\ldots,\sqrt{N} \times \sqrt{M}$. The input beamlet with the coordinate (n,m) is mapped to the output beamlet with the coordinate (m,n), called the transposition of the input. We can write as the equation:

$$(n,m) \rightarrow (m,n) \qquad (5)$$

The static OTIS composes of three stages of lenses. The microlenses in stage I are positioned one focal length away from the sources. The macrolens in stage II and microlenses array in stage III are positioned as shown in Figure 4(a) so that the images of the input beamlets can be Fourier transformed at the output. Figure 4(b) shows the diagram of the system for N and M = 16. The system is composed of 256 input and output beamlets arranged as a 4×4 array of 4×4 sub-arrays, a 4×4 array of lenses in stage I, a macrolens in stage II, and a 4×4 array of lenses in stage III. The input beamlet with coordinate $(1,1)$, for example, on the microlens n = 1 in stage I is mapped to the output beamlet with coordinate $(1,1)$ on the microlens n = 1 in stage III, similarly the input beamlet with coordinate $(1,2)$ on the microlens n = 1 in stage I is mapped to the output beamlet with coordinate $(2,1)$ on the microlens n = 2 in stage III, and so on.

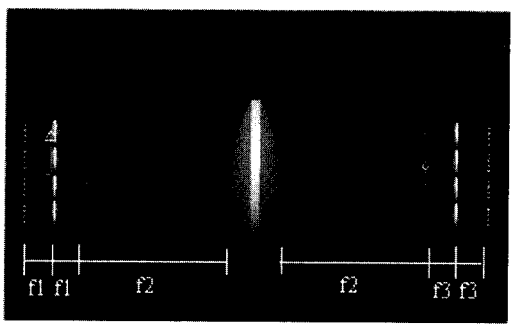

(a) Side View of the layout of the OTIS.

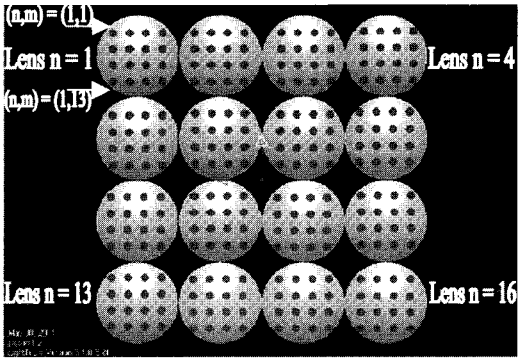

Coordinates of lenses and inputs in stage I

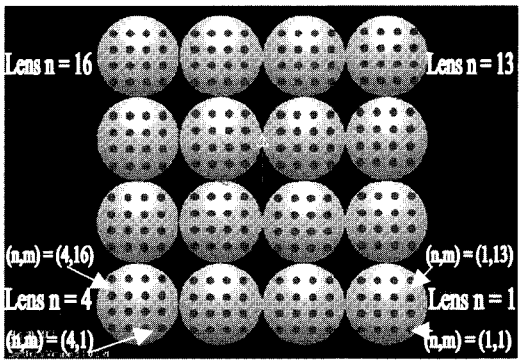

Coordinates of lenses and outputs in stage III
(b) Front View of inputs, outputs, and mesolenses in stage I and III.
Fig. 4. Diagram of the OTIS with $N = M = 16$.

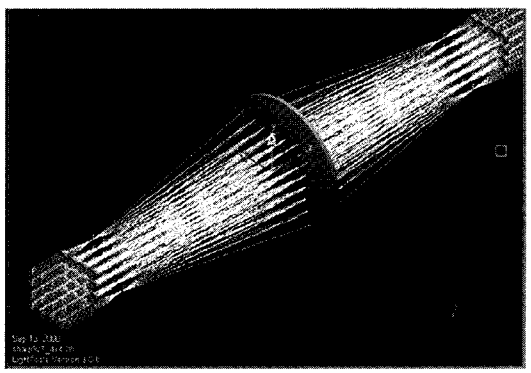

Figure 5. Modelling of the static OTIS.

The reconfigurable optical interconnection system proposed in this paper uses the optical superprism effect to control connecting patterns of optical interconnection. From Fig. 4 (a), each microlens in stage I is replaced with the group of the photonic crystals as shown in Fig. 6 and Fig 7.

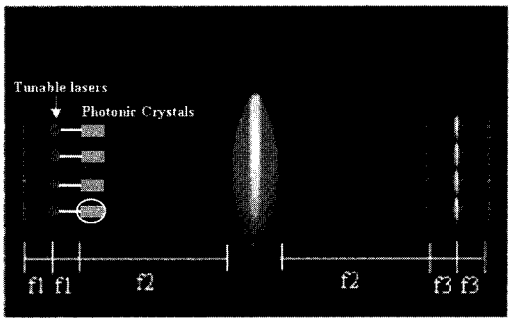

Fig. 6. New architecture of the reconfigurable optical interconnection system by replacing microlenses in stage I with the PC.

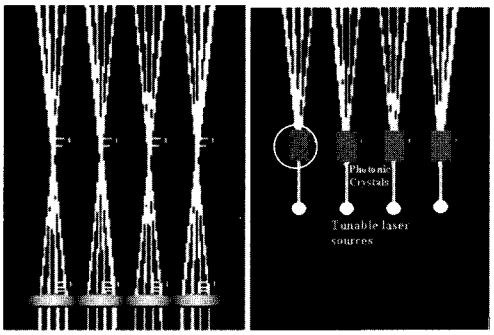

(a) (b)

Fig. 7. (a) Top view of the microlenses in stage I (in Fig. 5). (b) Replacing microlenses in (a) with the PC.

The position of each group of PCs is at the back focal point of the microlens in stage I of the static OTIS. Fig. 8 (a) shows that each group (in the circle) of the photonic crystal with the optical superprism effect in Fig. 7 (b) is composed of four 2-D photonic crystals. Each planar photonic crystal in Fig. 8 (a) has the top view as shown in Fig. 8 (b).

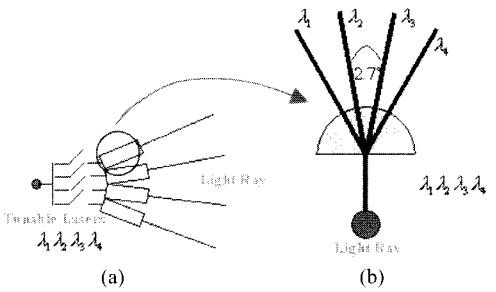

(a) (b)

Fig. 8. (a) Side view of the PC in circle in Fig. 6. (b) Top view of the PC with the optical superprism effect.

The light sources are tunable lasers with the wavelengths $\lambda_1, \lambda_2, \lambda_3$, and λ_4. By slightly

changing the incident wavelength over the wavelength range, light-beam steering in the PC's was achieved as shown in Fig. 3 and Fig. 8 (b). After replacing each microlens with the PCs, the 16 input beamlets arranged as an array (as shown in Fig. 4 (b)) will be decreased to a tunable laser source with on-off switch as shown in Fig. 7 (a) and (b). The angle between the deflected beams is 2.7°. If the tunable laser source is changed to λ_1 and only the top switch turns on, it will show that if the input beamlet at the coordinate (13,16) in Fig. 4 (b) is activated, the light ray will reach the output beamlet at (16,13). Another example: when the tunable laser source is adjusted to λ_1 and only the bottom switch turns on, if the input beamlet at the coordinate (4,1) is activated, the input beamlet will be transposed to the output beamlet at the coordinate (1,4). Fig. 9 shows a diagram of the reconfigurable optical interconnection system proposed in this paper.

The superprism effect in a photonic crystal is obtained by using simulation software, MIT Photonic-Bands (MPB) [13]. The 2-D planar photonic crystal is also designed by MPB software.

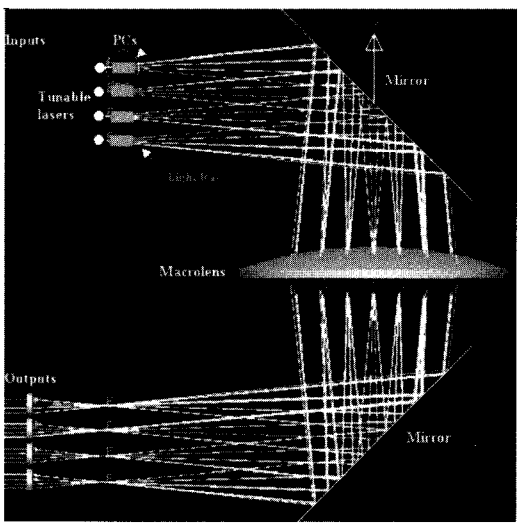

Fig. 9. The reconfigurable optical interconnection system based on the optical superprism effect in photonic crystals.

4. Conclusions

The reconfigurable optical interconnection system architecture proposed in this paper is a prototype of a 16×16 ($N\times M$) system. N and M, which are input ports and output ports respectively, can be expanded to 256×256 inputs and outputs by using the same optical system design. The system has a simple architecture compared to the conventional architecture which uses two arrays of micromirrors (MEMs) as shown in Fig. 10.

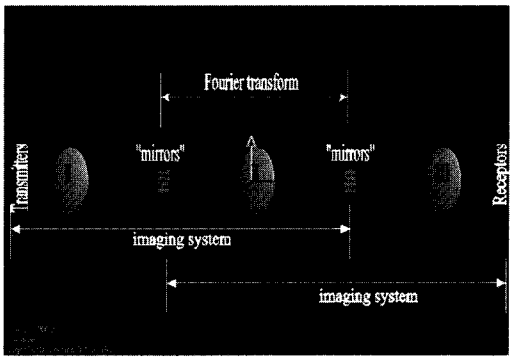

(a) The positions of the components.

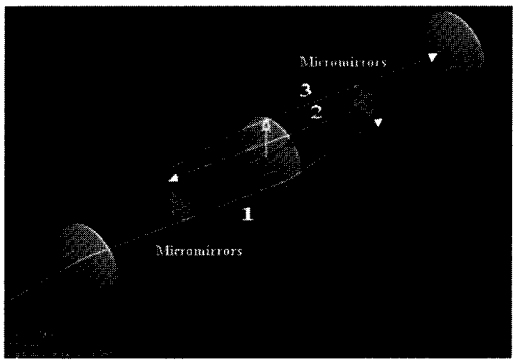

(b) Show the direction of light ray through the system starting from input to output.

Fig. 10. The conventional reconfigurable optical interconnection system using micromirrors (MEMs).

5. References

[1] C. S. Tocci and H. J. Caulfield ed. *Optical Interconnection: Foundations and Applications. '94*, Artech House Inc. 1994.

[2] H. Toshiyoshi, M. Kobayashi, D. Miyauchi, H. Fujita, J. Podlecki, and Y. Arakawa, *Design and analysis of micromechanical tunable interferometers for WDM free-space optical interconnection*, IEEE J. Lightwave Technol, Vol. 17, No. 1, pp. 19-25, 1999.

[3] John D. Joannopoulos, Robert D. Meade, and Joshua N. Winn, *Photonic Crystals: Molding the Flow of Light*, Princeton University Press, 1995.

[4] H. Kosaka, T. Kawashima, A. Tomita, M. Notomi, T. Tamamura, T. Sato, and S. Kawakami, *Superprism phenomena in photonic crystals: toward microscale Lightwave circuits*, IEEE J. Lightwave Tochnol, Vol. 17, No. 11, 2032-2038, 1999.

[5] T. Matsumoto and T. Baba, *Design and FDTD Simulation of Photonic Crystal k-Vector*, IEICE Trans. Electron, Vol. E87-C, No. 3, 393-397, 2004.

[6] T. Baba and T. Matsumoto, *Resolution of photonic crystal superprism*, Appl. Phys. Lett., Vol. 81, No. 13, 2325-2327, 2002.

[7] T. Baba and M. Nakamura, *Photonic crystal light deflection devices using the superprism effect*, IEEE J. of Quantum Electronics, Vol. 38, No. 7, 909-914, 2002.

[8] W. Pijitrojana and T. J. Hall, *Optical Transpose Interconnection System Architectures*, Thammasat Int. J. Sc. Tech., Vol. 8, No. 4, pp. 46-54, 2003.

[9] H. Kosaka, T. Kawashima, A. Tomita, M. Notomi, T. Tamamura, T. Sato, and S. Kawakami, *Photonic crystals for micro Lightwave circuits using wavelength-dependent angular beam steering*, Appl. Phys. Lett., Vol. 7, 1370-1372, 1999.

[10] H. Kosaka, T. Kawashima, A. Tomita, M. Notomi, T. Tamamura, T. Sato, and S. Kawakami, *Superprism phenomena in photonic crystals*, Phys. Rev. B, Vol. 58, No. 16, R10096-R10099, 1998.

[11] R. Zengerle, *Light propagation in singly and doubly periodic planar waveguides*, J. Mod. Opt., Vol. 34, No. 12, 1589-1617 1987.

[12] E. Silvestre, J. M. Pottage, P. St. J. Russel, and P. J. Roberts, *Design of thin-film photonic crystal waveguides*, Appl. Phys. Lett., Vol. 77, No. 7, pp. 942-944, 2000.

[13] MIT Photonic-Bands (MPB) Package is Free Software for Computing Band Structures (dispersion relations) of Optical Systems. The Package was Developed by Steven G. Johnson of the Joannopoulos Ab Initio Physics Group in the Condensed Matter Theory division of the MIT Physics Department.

Wanchai Pijitrojana received the B.Eng. degree in Telecommunication Engineering from King's Mongkut Institute of Technology, Ladkrabang, Bangkok, Thailand. He also received the M.S. degree in both, Computer Technology and Nonlinear Optics (Electrophysics) from the Asian Institute of Technology, Bangkok, Thailand and the University of Southern California, California, U.S.A., respectively, and the Ph.D. degree in Optoelectronics from King's College, University of London, London, England. He is currently a lecturer in the EE Department, Thammasat University, Bangkok, Thailand. His current research interests are Optical Interconnection systems, Optical Design, Optics, Nonlinear Optics, Physical Optics, PBG, and Mathematics applied to Optics.